BNL-96177-2011-JA

New Developments in Nb_3Sn PIT Strand: The Effects of Titanium and Second Phase Additions on the Superconducting Properties

L. R. Motowidlo, J. Distin, P. J. Lee, D. C. Larbalestier, and A. K. Ghosh

***Abstract*—We report the effect of titanium on the transport properties of multifilament PIT strand. In addition, the effect of second phase yttrium additions on the microstructure and the bulk pinning force are reported for PIT Nb_3Sn mono-core wires. High resolution SEM, EDS, magnetization, and transport measurements were utilized to evaluate the superconducting properties.**

***Index Terms*—Nb_3Sn mono-wire, powder-in-tube, titanium, yttrium second phase.**

I. Introduction

FOR magnet applications that require very high magnetic fields, there is a global push to develop superconductors with very high critical current density, J_c, coupled with a small effective filament diameter, D_{eff}, and high residual resistance ratio (RRR), $R_{300\,K}/R_{20\,K}$. At present, the only superconductor with the properties, availability, and price needed to operate in such high magnetic fields is Nb_3Sn [1].

An important issue is the high strain sensitivity of Nb_3Sn type superconductors. In the high magnetic field environment, the critical current properties may degrade significantly. Thus, to address these issues, improved conductor designs are needed [2].

We present latest results on continued developments on the Powder-In-Tube Nb_3Sn process (PIT) utilizing a novel octagonal architecture [3]. In this conductor design, octagonal PIT sub-elements allow the introduction of high strength components between the superconductor filaments in an efficient and uniform pattern. Fabrication of this novel design approach has been discussed in detail in an earlier publication [3]. The latest J_c properties of the octagonal PIT conductor design approach is presented in this paper.

Manuscript received August 27, 2010; accepted September 27, 2010. Date of publication November 29, 2010; date of current version May 27, 2011. This work was supported in part by the U.S. Department of Energy under Grant DE-FG02-06ER84920 (High Energy Physics). Work at BNL is supported by the U.S. Department of Energy under Contract DE-AC02-98CH10886. Additional support for work at NHMFL was provided by NSF Cooperative Agreement DMR-0084173 and by the State of Florida.

L. R. Motowidlo is with SupraMagnetics, Inc., Plantsville, CT 06479 USA (e-mail: LMOTO@cox.net).

P. J. Lee and D. C. Larbalestier are with the Applied Superconductivity Center at HMFL-FSU, Tallahassee, FL 32306 USA (e-mail: lee@asc.magnet.fsu.edu).

A. K. Ghosh is with Brookhaven National Laboratory, Upton NY 11973 USA (e-mail: aghosh@bnl.gov).

Color versions of one or more of the figures in this paper are available online at http://ieeexplore.ieee.org.

Digital Object Identifier 10.1109/TASC.2010.2089488

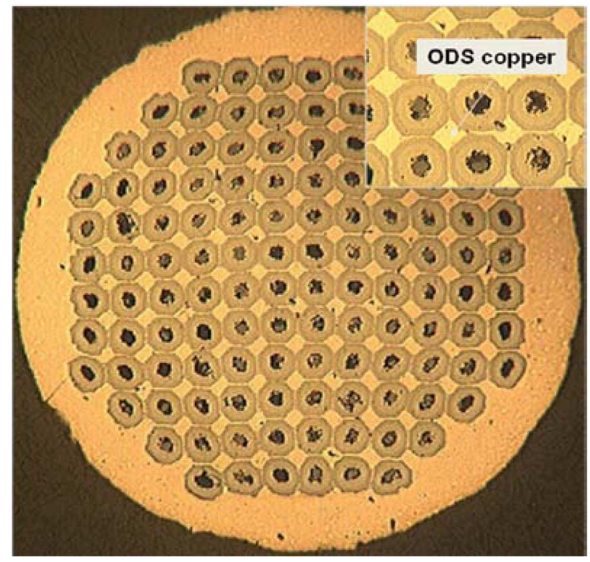

Fig. 1. A cross-section of the 120 octagonal PIT strand at 0.75 mm diameter after 650°C for 100 hours heat treatment. Filament diameter is 47 micron.

In addition, we present strand developments which explore the effect of titanium doping on superconducting properties in PIT strand and also the effect of second phase yttrium additions to the Nb_3Sn microstructure in monofilament wire.

II. Heat Treatment, H_K, and J_C Properties

Heat treatment optimization studies have been performed on the PIT octagonal conductor design shown in Fig. 1. Samples were heat treated from 625°C to 700°C. The optimum reaction temperature for this design was found to be 650°C for 100 hours to 200 hours for a 0.75 mm strand size. Increasing the time from 100 hours to 200 hours resulted in increasing the self field corrected Kramer field, H_k, from 24.81 T to 25.22 T. However, the non-Cu J_c decreased from 2458 A/mm^2 to 2430 A/mm^2 at 12 T. Further time increases to as long as 400 hours reduced the J_c to 2372 A/mm^2 and is presumably due to grain growth. A plot of transport non-Cu J_c versus the applied magnetic field to 12 T is shown in Fig. 2 for the optimum heat treatment of 650°C for 100 hours.

III. The Effect of Titanium on H_K

Over the last several years, the PIT process has become a viable approach for fabricating Nb_3Sn wires. The new PIT design of the conductor discussed above show promising performance characteristics for large scale magnet applications and has the potential for use in commercial magnets. In comparison to other

1051-8223/$26.00 © 2010 IEEE

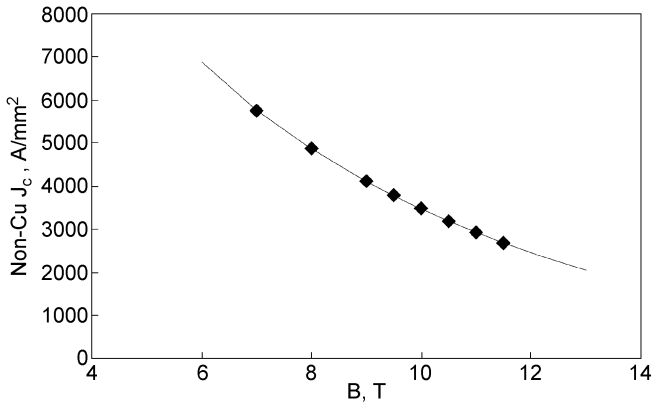

Fig. 2. The non-Cu J_c for the 120 octagonal PIT strand at 0.75 mm diameter after 650°C for 100 hours heat treatment.

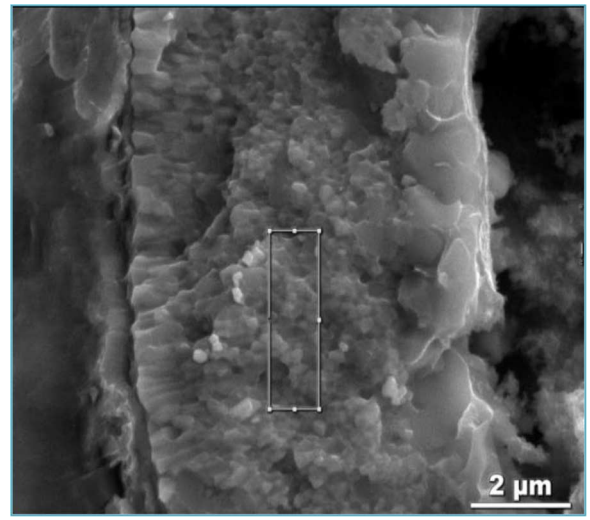

Fig. 3. High resolution micrograph of $(Nb, Ti)_3Sn$ A15 layer after 700°C heat treatment.

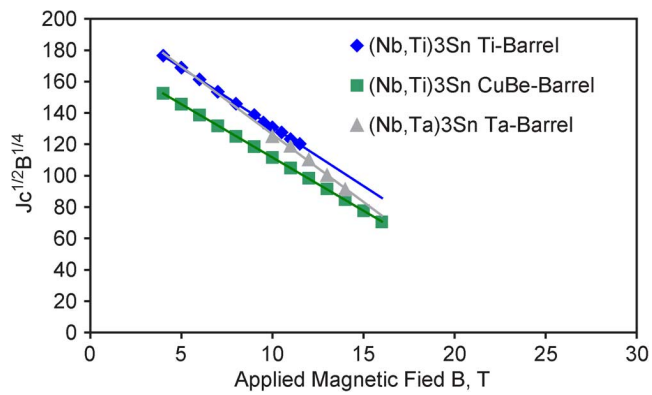

Fig. 4. Kramer plots for $(Nb, Ti)_3Sn$ and $(Nb, Ta)_3Sn$ PIT wires.

Nb_3Sn fabrication methods, the PIT process offers an efficient non-Cu package with no wasted copper [4] which has the potential for significant performance improvements [5]. Moreover, the PIT approach provides a flexible method of introducing additions via the core. For example, titanium may be introduced via the powder core to provide a source for the formation of the $(Nb, Ti)_3Sn$ superconductor. This is an advantage over other competing Nb_3Sn processes since off the shelf Nb1–2at% Ti alloy is not commercially available due to the inherent work hardening issues and wire breakage during processing [6].

In general, small amounts of 1–2at% Ti have shown improvement in the H_{c2} similar to that for Ta doping. In addition, J_c characteristics were better in the high field regime above 12 T [7]. State-of-the-art PIT Nb_3Sn have only been successfully fabricated with either Nb or Nb7.5wt%Ta tubes.

Earlier attempts of incorporating Ti into the A15 microstructure via the core have not been successful [8]. In this paper, we present the results of the first successful introduction of Ti into the A15 microstructure via a proprietary method. In Fig. 3, we show a high resolution micrograph of the fined grained A15 layer in a single filament of a 91 sub-element design. EDS analysis of a region depicted by the rectangle is shown in Fig. 3. The preliminary EDS analysis, in the A15 fine grained region suggest, a Ti level of about 1 to 2 atomic percent.

In order to evaluate the effect of the Ti on the properties in the PIT process, transport measurements were performed on strand with the Ti addition and compared to PIT strand with that of tantalum addition. Both were heat treated at 700°C for 100 hours. The A15 layer was measured utilizing a digital planimeter. The results were reduced in terms of the layer J_c in order to have a fair comparison of the properties, since the PIT strand design with titanium addition was not optimized for non-Cu J_c. In Fig. 4, Kramer plots for strand with Ti are compared to strand with Ta addition. The blue and green squares represent the $(Nb, Ti)_3Sn$ results with one sample measured on a Ti-Al-V barrel (blue diamond symbols) and the other on a Cu-Be type barrel (green square symbols). Also, the sample with the blue symbols was heat treated at 700°C while the sample with the green symbol was heat treated at 725°C. Both data show comparable Kramer slope. The results with the sample measured on the Cu-Be barrel showed lower performance characteristics, and this may be due to the higher heat treat temperature (725°C) for strand on the Be holder. Moreover, the Cu-Be holder likely puts the sample in greater compression compared to the titanium holder contributing to the lower J_c.

The results for the $(Nb, Ta)_3Sn$ strands are represented in Fig. 4 by the gray triangle symbols. In this case, the sample was mounted on a Ti barrel and heat treated at 700°C for 100 hours. The Kramer slope with increasing magnetic field of this sample is steeper than the Ti doped samples. The Kramer field, H_k, for each design was determined with no correction for self field. In the case of the $(Nb, Ta)_3Sn$ sample, the Kramer field was slightly less than 25 T. On the other hand, the $(Nb, Ti)_3Sn$ samples had a Kramer field exceeding 26 T. These results underscore the effect of the titanium addition in PIT type Nb_3Sn strand.

IV. The Efect of Y on the Superconducting Properties of PIT Mono-Filament Wires

It was pointed out by Cooley [9] that a global reduction of 0.3% in tin content produces a reduction by 18% of the value of the pinning force, F_p (12 T, 4.2 K). Thus, optimizing the composition of the Nb_3Sn reacted layer to ~25at% Sn can, in principle, yield an increase in J_c on the order of 40%–50% over

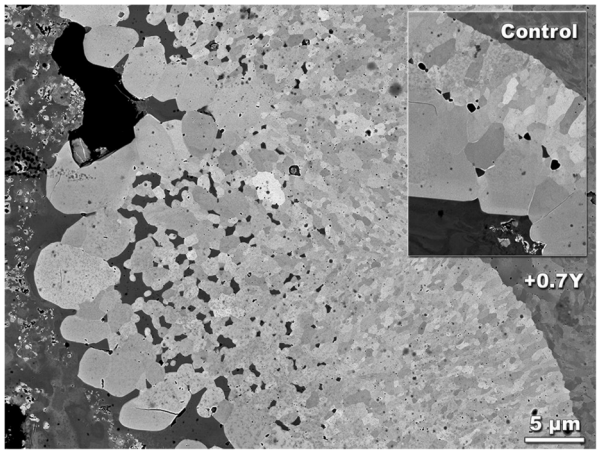

Fig. 5. High resolution micrographs of $(\mathrm{Nb7.5Ta0.75Y})_3\mathrm{Sn}$ after 850°C heat treatment. The inset compares the grain morphology of the $(\mathrm{Nb7.5Ta})_3\mathrm{Sn}$ control sample.

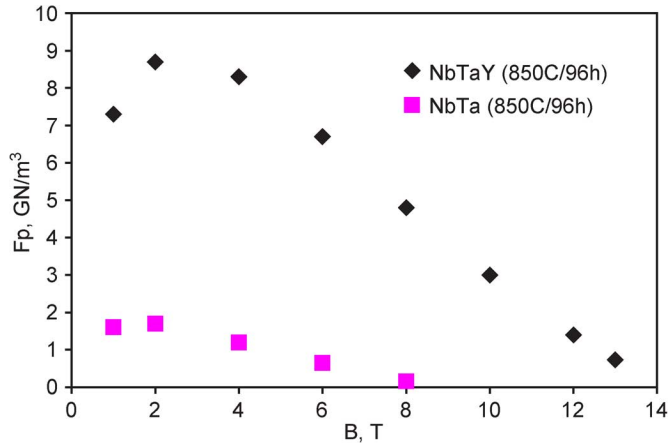

Fig. 6. The bulk pinning force versus the applied magnetic field for $(\mathrm{Nb,Ta})_3\mathrm{Sn}$ and $(\mathrm{Nb,Ta,0.75Y})_3\mathrm{Sn}$ at 9 K after 850°C heat treat.

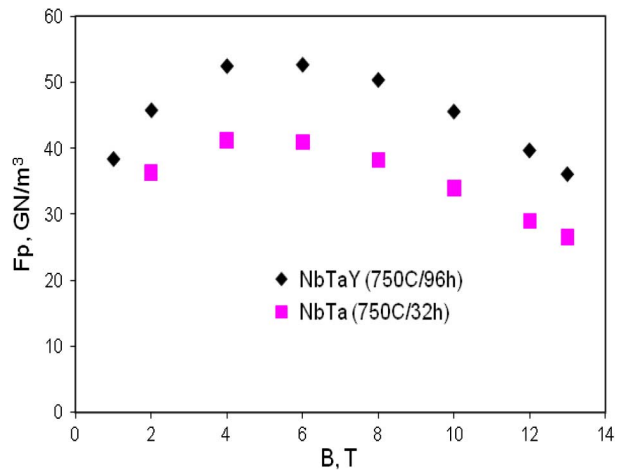

Fig. 7. The bulk pinning force versus the applied magnetic field for $(\mathrm{Nb,Ta})_3\mathrm{Sn}$ and $(\mathrm{Nb,Ta,0.75Y})_3\mathrm{Sn}$ at 4.2 K after 750°C heat treat.

current state-of-the-art PIT $\mathrm{Nb_3Sn}$ conductors. Heat treating at higher temperatures and longer times increases the average tin content closer to $\mathrm{Nb_3Sn}$ stochiometry and reduces T_c and H_{c2} gradients in the A15 layer. However, heat treatments at high temperatures invariably resulted in J_c reduction due to grain growth [10]. If the average grain size can be maintained below 150 nm and the tin content at ~25% uniformly across the layer, then an additional gain in J_c is expected.

In a previous paper, the addition of Gd and Y on the superconducting properties of $\mathrm{Nb_3Sn}$ mono-core wires was presented for the first time [11]. Preliminary results suggested possible improvements in suppressing grain growth at elevated heat treatments. In this paper, additional results are presented on PIT mono-wires fabricated with the addition of Y to the A15 microstructure. The fabrication of these mono-wires is described in the earlier publication [11].

A. The A15 Microstructure After 850°C Heat Treatment

As an example, high resolution SEM cross-section of the mono-wire with Y is shown in Fig. 5 after heat treatment at 850°C. The respective micrographs were positioned side-by-side to compare grain size. A discernable difference in grain size is observed. The large A15 grain region is clearly more prevalent in the control sample without yttrium doping. This is compared to the fine grain A15 region with the Y doped sample. The estimated grain size for the Y doped sample is 500 nm to 1000 nm. For the un-doped sample, the grains are 1 μm to 5 μm. This result suggests that the addition of 0.75 atomic percent yttrium may retard the A15 grain growth at higher temperatures of 750°C and 850°C.

V. The Bulk Pinning Force

The bulk pinning force was evaluated from magnetization measurements at 9 K and 4.2 K in applied magnetic fields to 12 T. Below, we present results after 750°C and 850°C heat treatment.

The superconducting area of each magnetization sample was measured by a digital planimeter. From the measurements, the effective inner and outer diameters, d_i and d_o respectively, of the A15 layer were determined. From the effective filament diameters and the width of the magnetization loop $\Delta\mathrm{M}$, the bulk pinning force $\mathrm{F_p}$ for the A-15 layer was calculated by the following relations [8]:

$$\Delta\mathrm{M} = (1/6) J_{cA15} nl \left[(d_o)^3 - (d_i)^3\right]$$
$$\mathrm{F_p} = J_{cA15} * B(\mathrm{T}) \quad (1)$$

where n in the present case represents one filament, l is the sample length, and J_{cA15} is the layer critical current density.

In Fig. 6, we compare the bulk pinning force curves with applied magnetic field for $(\mathrm{Nb,Ta})_3\mathrm{Sn}$ and $(\mathrm{Nb,Ta,0.75\%\ Y})_3\mathrm{Sn}$ samples at 9 K. In Fig. 7, a similar comparison is presented for the samples measured at 4.2 K after a reaction of 750°C/96 hrs.

For the Y-doped samples, an increase in the pinning force characteristics is observed at 9 K and 4.2 K. The maximum bulk pinning force $(\mathrm{F_{p\,max}})$ for the doped $(\mathrm{Nb,Ta})_3\mathrm{Sn}$ sample is about 55 $\mathrm{GN/m^3}$ at 4.2 K. This is compared to $\mathrm{F_{p\,max}}(4.2\ \mathrm{K})$ of about 40 $\mathrm{GN/m^3}$ determined by Fischer [10] after a 750°C heat treatment on PIT $\mathrm{Nb_3Sn}$ wire.

The smaller grain size in the yttrium doped sample may be partially responsible for the improvement in $F_{p\,max}$. In addition, the presence of the yttrium second phase particles themselves may be playing an important role in the pinning. Yttrium second phase discrete particles may be located inside the grains as well as in the grain boundaries, as observed in the starting ingots and described in the earlier paper [11].

VI. Summary

Nb_3Sn wires utilizing a novel octagonal PIT design show promising J_c characteristics in a high strength conductor configuration. Moreover, for the first time, the possibility of introducing titanium into the A15 matrix via the powder core has been successfully demonstrated. Preliminary results of titanium doping suggest that further improvements in the high field properties for PIT Nb_3Sn conductors are possible.

PIT Nb_3Sn mono-wires were fabricated with additions of second phase yttrium. These mono-wires were heat treated at 750°C and 850°C. In general, high resolution SEM showed smaller A15 grains in the doped Nb_3Sn mono-wires as compared to un-doped samples. The difference in grain size increased as the heat treatment temperature increased from 750°C to 850°C, indicating the grain boundary pinning effects of the second phase yttrium. Moreover, the large A15 grains typically found between the PIT core and the inner diameter of reacted Nb_3Sn layers were fewer and smaller in size in doped samples as compared to the control samples, heat treated under similar conditions.

Magnetization measurements performed at 9 K and 4.2 K showed improvements in F_p characteristics for yttrium doped samples. The increases in F_p may be due to a combination of flux pinning by grain boundaries and second phase particles. The results presented in this paper suggest a promising approach of incorporating non-alloying second phase yttrium within the A-15 layer that may reduce grain growth and hence improve the superconducting properties of PIT Nb_3Sn wires.

Acknowledgment

The authors thank Robert Neumann for the conductor processing and heat treatments, Van Griffin and Natanette Craig for electrical measurements, and Bill Starch for metallographic analysis. In addition, we would like to thank Najib Cheggour and Loren Goodrich for providing critical current data from their sample holder for comparison.

References

[1] R. M. Scanlan and D. R. Dietderich, "Progress and plans for the U.S. HEP conductor development program," *IEEE Trans. Appl. Super.*, vol. 13, no. 12, p. 1536, June 2002.

[2] J. W. Ekin, "Superconductors," in *Materials at Low Temperature*, R. P. Reed and A. F. Clark, Eds. Metals Park, Ohio: American Society for Metals, 1983, ch. 13, p. 465, 44073.

[3] L. R. Motowidlo, E. Barzi, D. Turrioni, N. Cheggour, and L. F. Goodrich, *IEEE Trans. Appl. Supercond.*, vol. 19, no. 3, p. 2598, June 2009.

[4] P. J. Lee *et al.*, "The microstructure and microchemistry of high critical current Nb_3Sn strands manufactured by the bronze, internal-tin, and PIT techniques," *IEEE Trans. Appl. Supercond.*, vol. 13, no. 2, p. 3422, 2001.

[5] A. Godeke *et al.*, "Possible improvements in Nb_3Sn wire properties via the reduction of inhomogeneities," in *LTSW*, Nappa Valley, California, 2002, unpublished.

[6] E. Gregory, *Private Communication.*.

[7] M. B. Field *et al.*, "Internal tin Nb_3Sn conductors for particle accelerator and fusion applications," *Advances in Cryogenic Engineering Materials*, vol. 54, p. 237, 2008.

[8] A. Godeke, A. den Ouden, A. Nijhuis, and H. H. J. ten Kate, *Cryogenics*, vol. 48, pp. 308–316, 2008.

[9] L. D. Cooley, C. M. Fischer, P. J. Lee, and D. C. Larbalestier, "Simulation of the effects of tin composition gradients on the superconducting properties of Nb_3Sn conductors," *Journal of Appl Phys.*, vol. 96, no. 4, p. 2122, 2004.

[10] C. M. Fischer, "," M.S. Thesis, University of Wisconsin, Madison, WI, 2002.

[11] L. R. Motowidlo, P. J. Lee, and D. C. Larbalestier, *IEEE Trans. Supercond.*, vol. 19, no. 3, p. 2568, 2009.